

Human glabrous skin contains crystallized urea dendriform structures in the *stratum corneum* which affect the hydration levels

Victor Hugo Pacagnelli Infante^{1,2} | Roland Bennewitz^{1,3} | Marius Kröger² |
Martina C. Meinke² | Maxim E. Darvin²

¹INM – Leibniz Institute for New Materials, 66123, Saarbrücken, Germany

²Department of Dermatology, Venereology and Allergology, Center of Experimental and Applied Cutaneous Physiology (CCP), Charité – Universitätsmedizin Berlin, Corporate Member of Freie Universität Berlin and Humboldt Universität zu Berlin, Charitéplatz 1, 10117, Berlin, Germany

³Department of Physics, Saarland University, 66123, Saarbrücken, Germany

Correspondence

Martina C. Meinke, Department of Dermatology, Venereology and Allergology, Charité – Universitätsmedizin Berlin, Charitéplatz 1, 10117 Berlin, Germany.
Email: martina.meinke@charite.de

Funding information

Volkswagen Foundation

Abstract

Glabrous skin is hair-free skin with a high density of sweat glands, which is found on the palms, and soles of mammals, covered with a thick *stratum corneum*. Dry hands are often an occupational problem which deserves attention from dermatologists. Urea is found in the skin as a component of the natural moisturizing factor and of sweat. We report the discovery of dendrimer structures of crystallized urea in the *stratum corneum* of palmar glabrous skin using laser scanning microscopy. The chemical and structural nature of the urea crystallites was investigated in vivo by non-invasive techniques. The relation of crystallization to skin hydration was explored. We analysed the index finger, small finger and tenar palmar area of 18 study participants using non-invasive optical methods, such as laser scanning microscopy, Raman microspectroscopy and two-photon tomography. Skin hydration was measured using corneometry. Crystalline urea structures were found in the *stratum corneum* of about two-thirds of the participants. Participants with a higher density of crystallized urea structures exhibited a lower skin hydration. The chemical nature and the crystalline structure of the urea were confirmed by Raman microspectroscopy and by second harmonic generated signals in two-photon tomography. The presence of urea dendrimer crystals in the glabrous skin seems to reduce the water binding capacity leading to dry hands. These findings highlight a new direction in understanding the mechanisms leading to dry hands and open opportunities for the development of better moisturizers and hand disinfection products and for diagnostic of dry skin.

KEYWORDS

glabrous skin, laser scanning microscopy, skin hydration, *stratum corneum*, urea

1 | INTRODUCTION

Glabrous skin is hair-free skin, which is found on the palms and soles. It is innervated by specialized nerves and presents a *stratum*

corneum (SC) whose thickness varies from 70 to 400 μm .^{1–4} It exhibits a high density of sweat glands, which appear as a helicoidal structure across the SC.⁵ Non-invasive optical techniques such as laser scanning microscopy (LSM) and confocal Raman microspectroscopy

This is an open access article under the terms of the [Creative Commons Attribution-NonCommercial-NoDerivs](https://creativecommons.org/licenses/by-nc-nd/4.0/) License, which permits use and distribution in any medium, provided the original work is properly cited, the use is non-commercial and no modifications or adaptations are made.

© 2023 The Authors. *Experimental Dermatology* published by John Wiley & Sons Ltd.

(CRM) have contributed to our knowledge in the investigation of the physiology of hairy skin, but rather few studies have applied these methods to glabrous skin⁶⁻⁹ because the optical access to lower skin layers is obstructed by the thick SC.

Dry hands are often observed in the population, where individual differences are found to be much larger than day-to-day differences.¹⁰⁻¹² This condition can affect the quality of life and is an occupational feature that deserves attention by dermatologists.¹² The mechanisms leading to dry hands are still unclear.¹¹ Additional knowledge about the constitution of glabrous skin is needed to address this challenge for earlier diagnostic and to open new pathways in the development of moisturizers.

Urea is a polar, hygroscopic molecule which is produced endogenously by the human body metabolism.¹³⁻¹⁵ It is excreted with sweat and is naturally found in the skin.^{16,17} Urea plays an important physiological role in the SC homeostasis, representing $\approx 7\%$ of the natural moisturizing factor (NMF) composition.^{13,14} It contributes to the hygroscopic capacity but also to the keratolytic function. Urea binds water and dissolves keratin and is therefore utilized as a humectant agent in commercial hand moisturizers.¹⁸

In LSM images recorded *in vivo* of the glabrous skin we discovered crystallized urea dendriform (CUD) structures located exclusively in the SC, which to the best of our knowledge were not described previously in the literature. We performed a comprehensive analysis using different non-invasive optical methods and determined the chemical nature and morphology of CUD structures. We correlate the urea crystal formation to the measured skin moisture of participants and discuss the possible role of crystalline urea for the moisture level.

2 | MATERIALS AND METHODS

2.1 | Volunteers and study protocol

Eighteen volunteers (7 males, 11 females) aged from 23 to 62 years (average 38 ± 12 years) were enrolled in this study. The volunteers were instructed to not apply any cosmetic formulation such as moisturizers and disinfection lotions to the hands for at least 24 h prior to the study. The participants did not wash their hands in the 15 min before the first measurements. High-resolution images were recorded by LSM in the skin of index and small fingers as well as the tenar palm area. Skin hydration was also evaluated in these areas. Eight volunteers were selected for CRM measurements, three of them did not show CUD in LSM images. Three participants with CUD structures were selected for the two-photon tomography measurements. This study was approved by the Committee of Ethics in Research Involving Human Subjects (EA1/114/22) and performed in accordance with the ethical standards of the Declaration of Helsinki, as revised in 2013. The participants of this study have given written informed consent to publication of their data. The study was conducted during winter. Before the measurements, participants acclimated to an environment with controlled air temperature and relative humidity (20–22°C and 45%–55%) for 15 min.

2.2 | Skin hydration

We utilized a skin capacitance meter (Corneometer™ CM 825, Courage & Khazaka Electronic GmbH, Cologne, Germany) *in vivo* which determines the water content in the superficial SC and expresses the values in arbitrary units. The average values of 5 measurements per site were used in subsequent analyses.¹⁹

2.3 | Laser scanning microscopy (LSM)

Non-invasive *in vivo* skin images were recorded with a confocal laser scanning microscope (VivaScope® 1500 Multilaser, Mavig, Germany, 785 nm laser). The scanned area measures $500 \mu\text{m} \times 500 \mu\text{m}$, producing images of $1000 \text{ pixels} \times 1000 \text{ pixels}$.^{20,21} A series of consecutive reflectance LSM images started from the skin surface up to $200 \mu\text{m}$ in depth, separated by $4.5 \mu\text{m}$ increment (Vivastack® Mavig, Germany). Images were analysed using Image J software.²² To study the spatial distribution of the SC structures, mosaics of high-resolution $500 \mu\text{m} \times 500 \mu\text{m}$ images were taken in a depth of 50 to $75 \mu\text{m}$ and composed into LSM images of $3 \text{ mm} \times 3 \text{ mm}$ (Vivablock®).

To calculate the relative CUD volume, we analysed the VivaStack images, in which the CUD structures appear as very bright reflectance signal with a saturated grey level of 255. The area containing CUD was calculated by setting a grey index threshold to 254. The absolute CUD volume was then calculated as the sum of all areas for each image according to the depth. The relative volume content of CUD reported below was determined by dividing the absolute CUD volume by the SC depth of analysed images with CUD. Three-dimensional representations of the CUD shapes were created by interpolating the images in ImageJ using 8bit images.

2.4 | Confocal raman microspectroscopy (CRM)

Measurements were performed *in vivo* with a confocal Raman microscope (Model 3510, RiverD International B.V.) at 785 nm excitation for acquisition in the fingerprint region (FP, $400\text{--}2000 \text{ cm}^{-1}$, exposure time 5 s, 20 mW) and at 671 nm excitation for the acquisition in the high wavenumber region (HWN, $2000\text{--}4000 \text{ cm}^{-1}$, exposure time 1 s, 17 mW).²³

Raman spectra in the FP and HWN regions were recorded at the same lateral position between a height of $5 \mu\text{m}$ above the skin surface and $60 \mu\text{m}$ below the surface in increments of $2 \mu\text{m}$. For determination of the water, NMF and urea concentration profiles, measurements were carried out to a depth of $120 \mu\text{m}$ with $4 \mu\text{m}$ increment.

2.5 | Calculation of dissolved urea and water content in the SC

The relative concentration of urea was determined by classical least squares fitting, using the “SkinTools 2.0” software (RiverD

International B.V.). A set of reference spectra of the major skin constituents was fitted to the Raman spectra. The fit coefficients were normalized by the signal from keratin, which is the dominant dry mass fraction in the SC. The water concentration depth profiles in the SC were determined using the same software. The calculation is based on the intensity ratio of the water-related OH vibration ($3350\text{--}3550\text{ cm}^{-1}$) to the vibration of keratin ($2910\text{--}2965\text{ cm}^{-1}$),²⁴ which is precisely determined in the skin. The calculation of skin molecules such as urea is based on amplitudes and spectra of the eight basic components that contribute significantly to the $800\text{--}1800\text{ cm}^{-1}$ range of the Raman spectrum as described previously.²⁵

2.6 | Calculation of the ratio dissolved/crystallized urea forms using CRM

The concentration of the urea dissolved in water was calculated from Raman spectra. The band at 1004 cm^{-1} is specific for diluted urea in skin, while the band at 1010 cm^{-1} is specific for crystallized urea. We calculated a I_{1004}/I_{1010} band ratio to estimate the differences in the relation between dissolved and crystallized urea for the participants. For calibration, we performed Raman microspectroscopy in-vitro on a solution of urea and on crystals of urea and observed the shifting of bands located between 1000 and 1012 cm^{-1} for dissolved and crystallized urea.

2.7 | Two-photon tomography

A two-photon tomograph (Dermaininspect, JenLab GmbH) equipped with a tunable femto-second Ti: sapphire laser (Mai Tai XF, Spectra Physics) operated at 760 nm excitation and 100 fs pulses at a repetition rate of 80 MHz , was used for horizontal imaging of glabrous human skin in vivo.^{26,27}

For 760 nm excitation, a $410\text{--}680\text{ nm}$ band pass filter was used to detect two-photon excited autofluorescence (TPE-AF) and a $375\text{--}385\text{ nm}$ band pass filter was applied to detect the second harmonic generation (SHG) signal, which is specific to non-centro-symmetric structures.^{28,29}

To analyse if the surfaces of pure crystals of urea cause second harmonic generation, 0.2 mg of pure urea was dissolved in 1 mL of distilled water. After agitation, $10\text{ }\mu\text{L}$ of this solution was placed in a microscopy lamina. Urea crystals were observed after water evaporated and investigated with the two-photon tomography.

2.8 | Statistical analysis

The Shapiro-Wilk test was used to evaluate the normality of distributed data. When normality was determined, ANOVA or t-test was used to test significant differences ($\alpha=0.05$). The analyses were carried out with the software Prism GraphPad 8.4.3. $p\leq 0.05$ was settled as "significant". All values in the figures are plotted with the mean values \pm standard deviation.

3 | RESULTS AND DISCUSSION

3.1 | Morphological characterization of CUD structures using LSM

During the LSM examinations of the glabrous skin, we discovered structures with high reflectance in the SC, presenting a dendriform constitution and reminding of crystals (Figure 1). We will refer to them as crystalline urea dendriform (CUD) structures.

The size of the CUD structures is variable with different spatial organizations. Normally, they assume an elongated core shape with attached small arms of a length from 2 to $15\text{ }\mu\text{m}$. These arms are not connected with other CUD structures (Figure 1A). The example LSM images presented in Figure 1A were obtained from palm, index finger and small fingers of participants 002, 009 and 013 (Table 1). In these images, longer dendritic arms are also observed which connect different CUD structures, creating a chain which may extend across the SC. CUD structures were observed only in the SC, and preferentially close to its surface. For a visualization of the shape and distribution of CUDs in the SC refer to the 3D models in the supplementary files (Figures S1 and S2, obtained from the palm of participant 013). The average density of CUD structures for all the participants decreases from the surface to the bottom of the SC (Figure 1B).

To the best of our knowledge, the CUD structures have neither been reported for the glabrous skin nor for the hairy skin. In this study, hairy skin was not investigated since extensive experience of the authors with LSM imaging has never suggested any CUD structures in hairy skin.

The CUD structures present a high reflectance in LSM, so that the area of CUD structures within an image could be determined by counting pixels with a Grey Index Level (GIL) of 254 or 255, the maximum level. No other significative structure in the SC presents those high values of reflectance in the images, except some sweat glands whose area was subtracted during the evaluation (Figure 1C–G). Some very small areas may also present this very high reflectance, especially next to the ridges, resulting in a very small quantification of reflectance for participants without CUD (Figure S3).

For participant P002 we have performed the LSM in the sole from the right foot and we have observed a small amount of CUD (Figure S4). We believe that the presence of CUD structures is not too frequent in the soles since we are constantly using closed shoes and socks which are able to retain skin hydration, which keeps urea in solution.

3.2 | Presence of CUD structures and participant data

The diverse morphologies presented in Figure 1 demonstrate a variation of CUD structures between anatomic regions and between individual participants. All information regarding anatomic region tested, age, sex, presence of CUD structures, thickness of SC and of viable epidermis, and the SC hydration are summarized in Table 1.

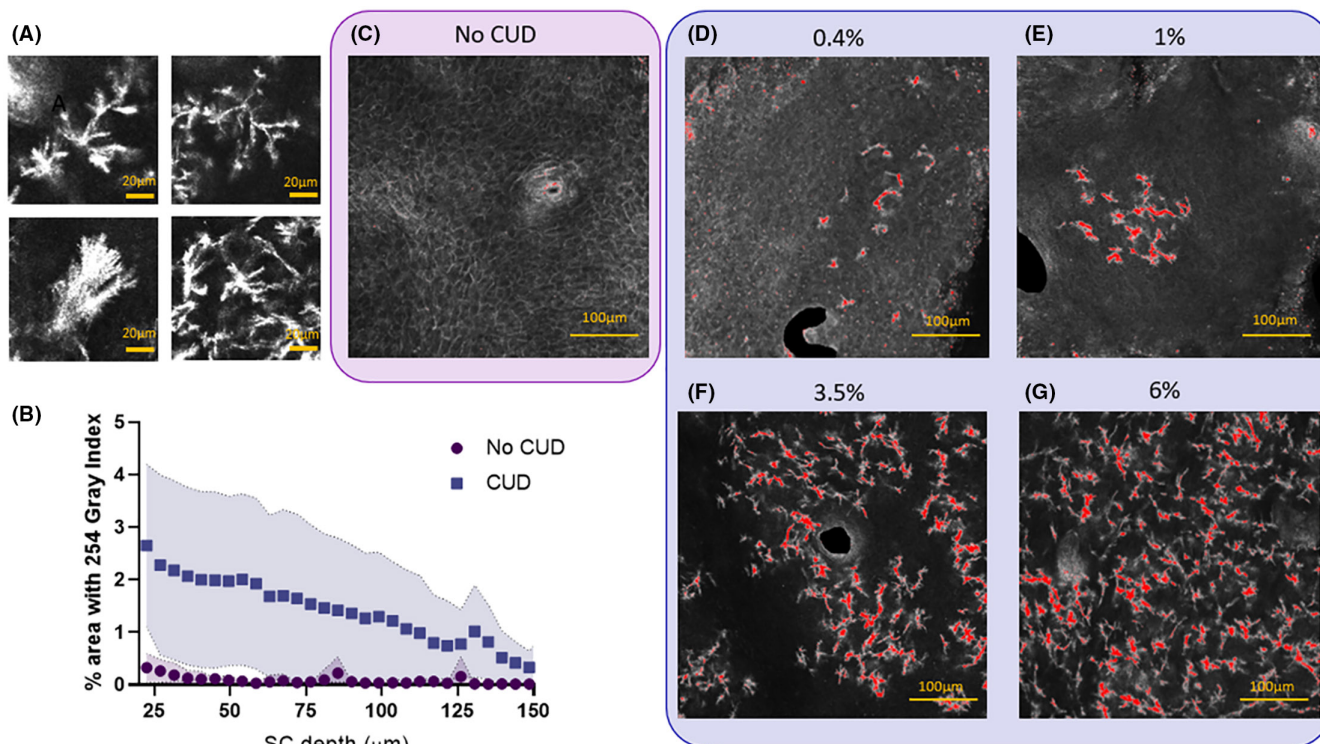


FIGURE 1 In vivo LSM images of human glabrous skin regions containing CUD structures. Images in A represent the diverse morphological shapes of the CUD structures in the SC observed in different anatomic regions of different individuals. The graphic in B presents the depth distribution of CUD structures according to the *stratum corneum* depth. Image C is a stack recorded of an individual not showing any CUD structures. Images D to G show glabrous skin with different amounts of CUD structures. Red colour indicates a grey level index of 254 or 255 and thus the presence of CUD structures; it was included artificially in the images using ImageJ software.

We observed CUD structures in 13 of 18 participants, mostly in all three anatomic regions tested, but also only in one or two of them. Some participants exhibit CUD structures in the palm but not in the fingers. Generally, CUD structures are more prominent in the palm if compared with fingers, where a smaller number of isolated structures are observed frequently. Since the number of participants is small, we cannot affirm influences of sex or age, however, a stronger presence of CUD was observed in participants more than 30 years old with a tendency to increase even more the volume for the participants with more than 40 years old and CUD.

The volunteers were asked about their use of cosmetics. Nine participants reported the daily use of hand moisturizing creams, six applying creams containing urea and three creams not containing urea. Three participants who normally apply cream with urea did not present CUD structures in the glabrous skin.

3.3 | Crystalline structure of urea dendriform

Two-photon tomography provides additional information about the constituents of skin layers. We observed a strong SHG signal, whose shape and localization coincide with the CUD structures in previously recorded LSM images (Figure 2E–G). The SHG is a strong indication for presence of crystalline material, since SHG is most

effective at the non-centrosymmetric surfaces of crystals. In skin, only collagen type I has been reported to provide SHG.³⁰ We have prepared crystalline urea in vitro for comparison and could confirm the surface sensitivity of our SHG experiment in the detection of urea crystallization (Figure 2H). Urea is one of the commercially available crystalline substances that exhibit strong optical nonlinearity and is well known for SHG.^{31–34} Thus, the contrast in SHG images of the SC indicates the dendriform crystalline structure of the urea.

3.4 | Comparing *stratum corneum* with and without CUD structures by confocal Raman microspectroscopy

The chemical and crystalline nature of the CUD structures was further confirmed by CRM. This analysis included six anatomic regions without CUD structures from three participants, six regions with a few isolated CUD structures from three participants, and twelve regions with dense CUD structures from five participants.

The most prominent difference between regions with and without CUD structures was the urea content in the SC. Participants without CUD structures exhibited 2 to 4 times higher urea signal in CRM (Figure 3A). Participants without the CUD exhibited a significantly increased water content for the top 50 µm of the SC. The first

TABLE 1 Information for each participant and anatomic position.

Participant and anatomic position	Sex/Age	SC thickness(AV \pm SD μ m)	Presence of CUD?	SC moisture(Arb. Unit.)	Volume fraction of CUD
001 IF	F/29	214 \pm 22	Yes	81 \pm 5	0.10
001 SF		164 \pm 7	Yes	87 \pm 3	0.07
001 PL		159 \pm 7	No	49 \pm 3	-
002 IF		233 \pm 13	No	69 \pm 7	-
002 SF	M/30	157 \pm 17	Yes	52 \pm 3	0.35
002 PL		89 \pm 9	Yes	35 \pm 1	0.39
003 IF		208 \pm 7	No	43 \pm 2	-
003 SF	F/56	179 \pm 9	No	56 \pm 3	-
003 PL		119 \pm 10	No	42 \pm 5	-
004 IF		128 \pm 6	Yes	60 \pm 3	0.37
004 SF	F/26	96 \pm 14	Yes	67 \pm 3	-
004 PL		90 \pm 5	Yes	45 \pm 3	0.19
005 IF		240 \pm 17	No	114 \pm 4	-
005 SF	M/28	210 \pm 23	No	112 \pm 2	-
005 PL		144 \pm 28	No	92 \pm 5	-
006 IF	M/30	290 \pm 13	No	66 \pm 6	-
007 IF		180 \pm 22	Yes	77 \pm 9	0.17
007 SF	F/39	141 \pm 12	No	66 \pm 6	0.20
007 PL		102 \pm 9	Yes	37 \pm 3	0.12
008 IF		208 \pm 12	No	83 \pm 3	-
008 SF	M/44	170 \pm 9	Yes	99 \pm 2	0.06
008 PL		116 \pm 5	No	64 \pm 2	-
009 IF		170 \pm 27	Yes	56 \pm 5	0.41
009 SF	F/61	140 \pm 15	Yes	53 \pm 7	0.48
009 PL		115 \pm 5	Yes	35 \pm 2	0.45
010 IF		211 \pm 4	No	61 \pm 5	-
010 SF	M/32	123 \pm 12	No	88 \pm 6	-
010 PL		102 \pm 5	Yes	48 \pm 6	0.21
011 IF		187 \pm 15	Yes	79 \pm 2	0.11
011 SF	F/53	161 \pm 13	Yes	92 \pm 7	0.08
011 PL		129 \pm 6	Yes	29 \pm 3	0.43
012 IF		198 \pm 18	No	72 \pm 3	-
012 SF	F/33	126 \pm 9	Yes	96 \pm 7	-
012 PL		102 \pm 5	Yes	45 \pm 3	0.12
013 IF		196 \pm 10	Yes	34 \pm 2	0.52
013 SF	F/37	158 \pm 21	Yes	64 \pm 3	0.27
013 PL		131 \pm 5	Yes	38 \pm 6	0.32
014 IF		154 \pm 14	Yes	52 \pm 5	0.42
014 SF	F/62	122 \pm 21	Yes	60 \pm 2	0.36
014 PL		110 \pm 14	Yes	23 \pm 1	0.61
015 IF		154 \pm 15	Yes	69 \pm 6	0.19
015 SF	F/26	126 \pm 11	Yes	69 \pm 4	0.13
015 PL		98 \pm 5	Yes	38 \pm 2	0.2
016 IF		178 \pm 14	No	61 \pm 5	-
016 SF	F/32	122 \pm 6	No	70 \pm 3	-

TABLE 1 (Continued)

Participant and anatomic position	Sex/Age	SC thickness(AV ± SD μm)	Presence of CUD?	SC moisture(Arb. Unit.)	Volume fraction of CUD
016 PL		105 ± 4	No	44 ± 7	-
017 IF		265 ± 4	No	95 ± 4	-
017 SF	M/23	203 ± 14	No	90 ± 4	-
017 PL		124 ± 13	No	64 ± 9	-
018 IF		208 ± 14	Yes	21 ± 4	0.53
018 SF	M/50	184 ± 10	Yes	27 ± 3	0.76
018 PL		144 ± 5	Yes	25 ± 5	0.81

Abbreviations: IF, Index Finger; SF, Small Finger; PL, Palm.

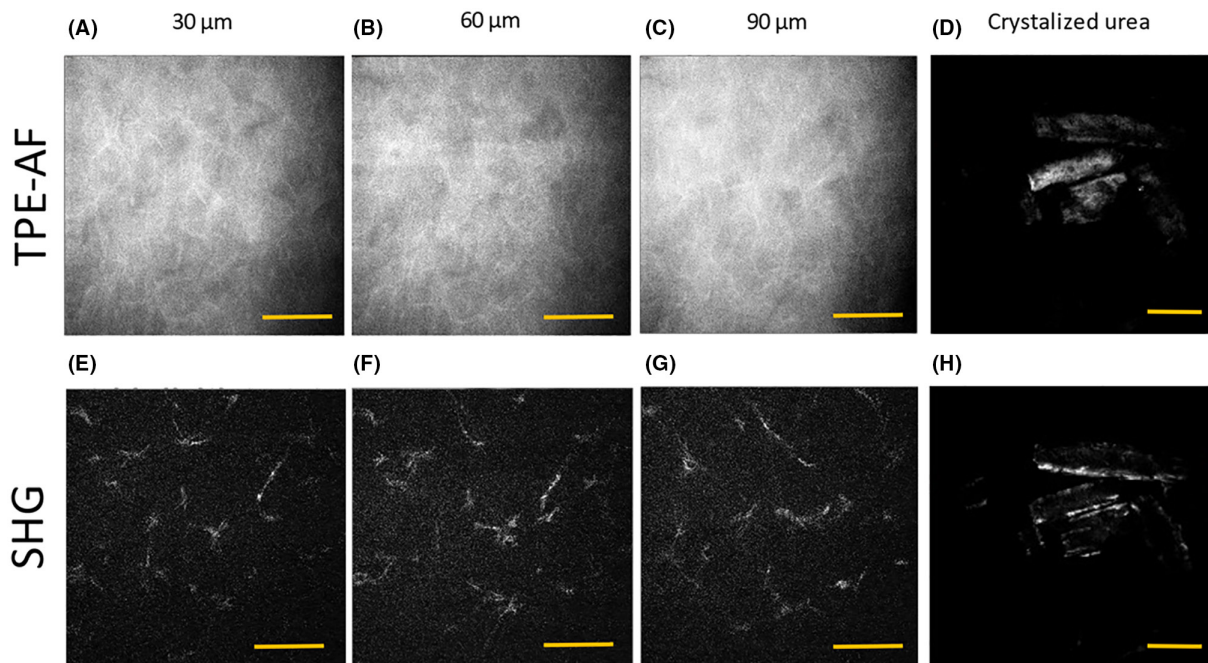


FIGURE 2 In vivo MPT (multi photo tomography) images of the human palm tenar region containing CUD structures. Two-photon excited autofluorescence (TPE-AF) and SHG (second harmonic generation) images of the SC recorded in vivo in depths of 30, 60 and 90 μm (A–C and G–E) are compared with those of in vitro crystallized urea (D and H). Scale bars represent 30 μm.

40 μm SC depth contain up to 45% of water and these values slightly decrease with increasing SC depth, however they are always higher than 35% (Figure 3B). The NMF was also reduced for the volunteers with the CUD (Figure 3C).

Comparing crystals of urea and solution of urea in Raman spectroscopy, we observed a shift from 1004 to 1010 cm⁻¹ in the characteristic Raman band (Figure 3D). For SC without CUD structures, the Raman band in this range resembles the narrow band of urea in solution at 1004 cm⁻¹. However, for participants with CUD structures, the Raman band is a superposition of the band for dissolved urea and for the crystalline urea with intensity at 1010 cm⁻¹ (Figure 3D).

The CRM is a well-established method to analyse water and urea concentration in the SC.^{24–26} The Raman band at 1004 cm⁻¹ is specific to dissolved urea. This urea-related Raman band overlaps with

the band characteristic for phenylalanine.^{35–37} Upon crystallization, the urea-related band at 1004 cm⁻¹ shifts towards higher wavenumbers to 1010 cm⁻¹ (Figure 3D). This band is assigned to symmetrical CN stretching vibrations which shift towards higher wavenumbers in the solid state.^{36–38} We observe for SC with CUD structures a reduction in the 1004 cm⁻¹ band intensity (I_{1004}) and an increase in the 1010 cm⁻¹ band intensity (I_{1010}) as a shoulder in the Raman spectrum (Figure 3D). According to these findings and the SHG signals reported previously, we conclude that the CUD structures are indeed comprised of crystalline urea. We do not expect a complete reduction of the 1004 cm⁻¹ band intensity because some urea will remain dissolved in the SC and because this band also represents the presence of phenylalanine. The distribution of the 1010 cm⁻¹ band intensity across the SC depth indicates a non-homogeneous distribution

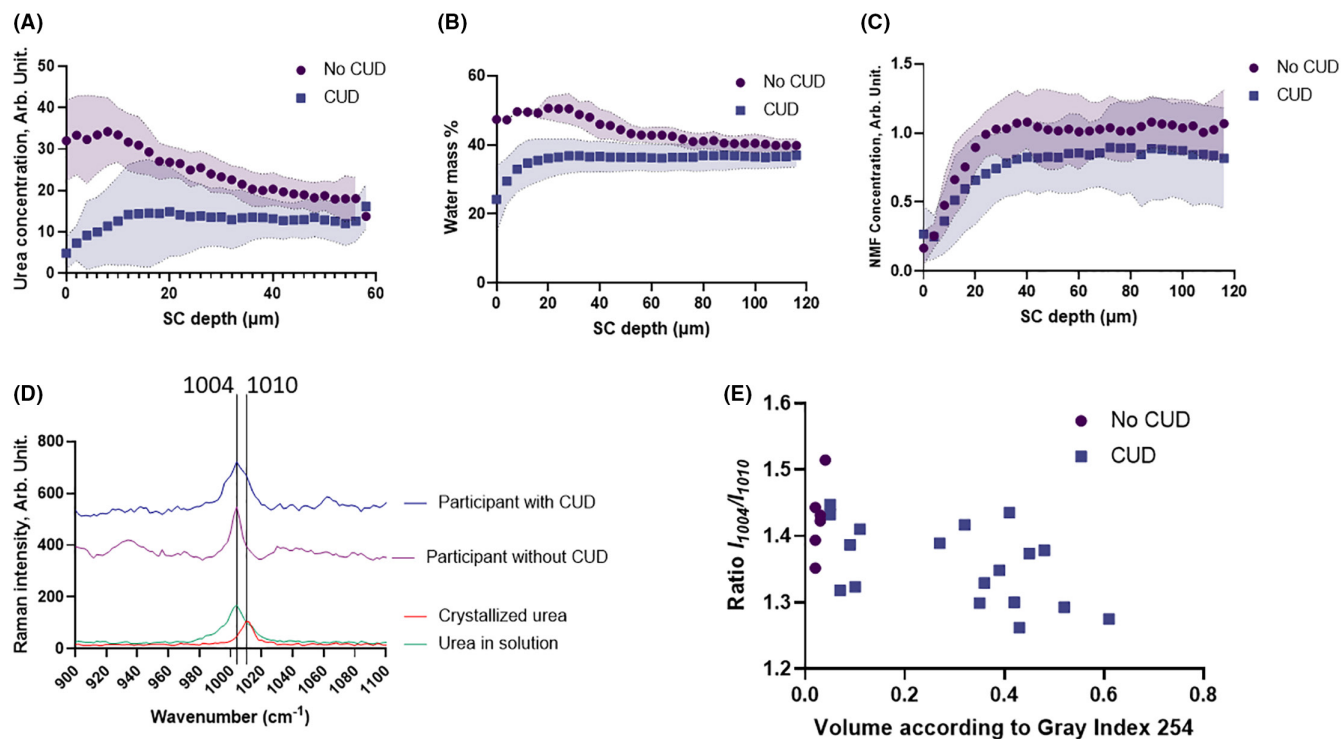


FIGURE 3 In vivo CRM evaluation of urea, water and NMF distribution in the glabrous skin and evidence for the presence of urea in the crystallized form. Distribution of urea concentration (A), water mass (B) and NMF (C) for SC with and without CUD structures determined by CRM. Raman spectra for SC with CUD structures, without CUD structures, in vitro dissolved and crystallized urea, respectively, with the bands at 1004 and 1010 cm^{-1} which are characteristic for dissolved or crystallized urea (D). The I_{1004}/I_{1010} ratio was negatively correlated ($R^2 = -0.35$, $p = 0.002$) to the volume fraction of CUD structures (E).

of CUD structures, but also the attenuation of the Raman signal intensity with increasing depth.

The I_{1004}/I_{1010} ratio indicates the relation between diluted and crystallized urea. For the SC with a high amount of CUD structures, a reduction in the I_{1004}/I_{1010} ratio was observed, representing an increase of urea crystallization compared to SC showing no CUD structure. Summarizing all measurements, the I_{1004}/I_{1010} ratio has a negative correlation with the volume fraction of CUD structures ($R^2 = 0.35$; $p = 0.002$) (Figure 3E).

Other studies also observed the presence of the band at 1010 cm^{-1} for crystalline urea and applied it to the study of creams containing urea. Egawa and Sato³⁶ observed the deposition of urea crystals in the volar arm skin of women after the utilization of a 20% urea cream. It was found in the superficial SC depth, where the water content is below 50% and the band at 1010 cm^{-1} is strongly pronounced. Goto et al.³⁹ observed Raman bands shifted to 1012 cm^{-1} for formulations which deposit high amounts of urea crystal in the skin surface.

It is also interesting to note that the stability of urea creams is a classical challenge in the cosmetic and pharmaceutical industries.^{13,36,39} Urea is sensitive to variations in the lipidic-hydrophilic balance of the formulations as well as to the pH value. The initial concentration of urea and the utilization of other humectants in the formulation are fundamental for the design of stability strategies. The crystallization tendency of urea already observed in cosmetics

is a starting point to understand mechanisms for the same process in a lamellar structure such as the SC.

3.5 | Glabrous skin hydration

The small finger is more hydrated than the index finger (SF 80 ± 18 Arb. Unit versus IF 68 ± 21 Arb. Unit, $p = 0.006$) and the palm exhibits significantly lower moisture compared with the other anatomic regions which were analysed in this study (PL 44 ± 17 Arb. Unit, $p < 0.001$). Anatomic regions with CUD structures have a lower skin hydration value than regions without CUD structures (Figure 4). SC with CUD structures exhibits a reduction in the skin hydration, which is negatively correlated with the volume fraction of CUD structures (Figure 4, $R^2 = 0.55$; $p < 0.001$). The lower moisture value of the palm is in agreement with the higher number of CUD in this anatomic position. In support of this statement, volunteer P018 reported the very dry hands, had very low skin hydration (Table 1) and the highest concentration of CUD (Figure 4).

Urea is delivered to the SC by two independent pathways: by the physiological keratinocyte proliferation cycle which accumulates urea inside the corneocytes, and by excretion from the sweat glands. Both pathways may contribute to the formation of crystallized urea by saturating both intercellular and intracellular space in the superficial SC.^{10,40-42} The water concentration in the superficial

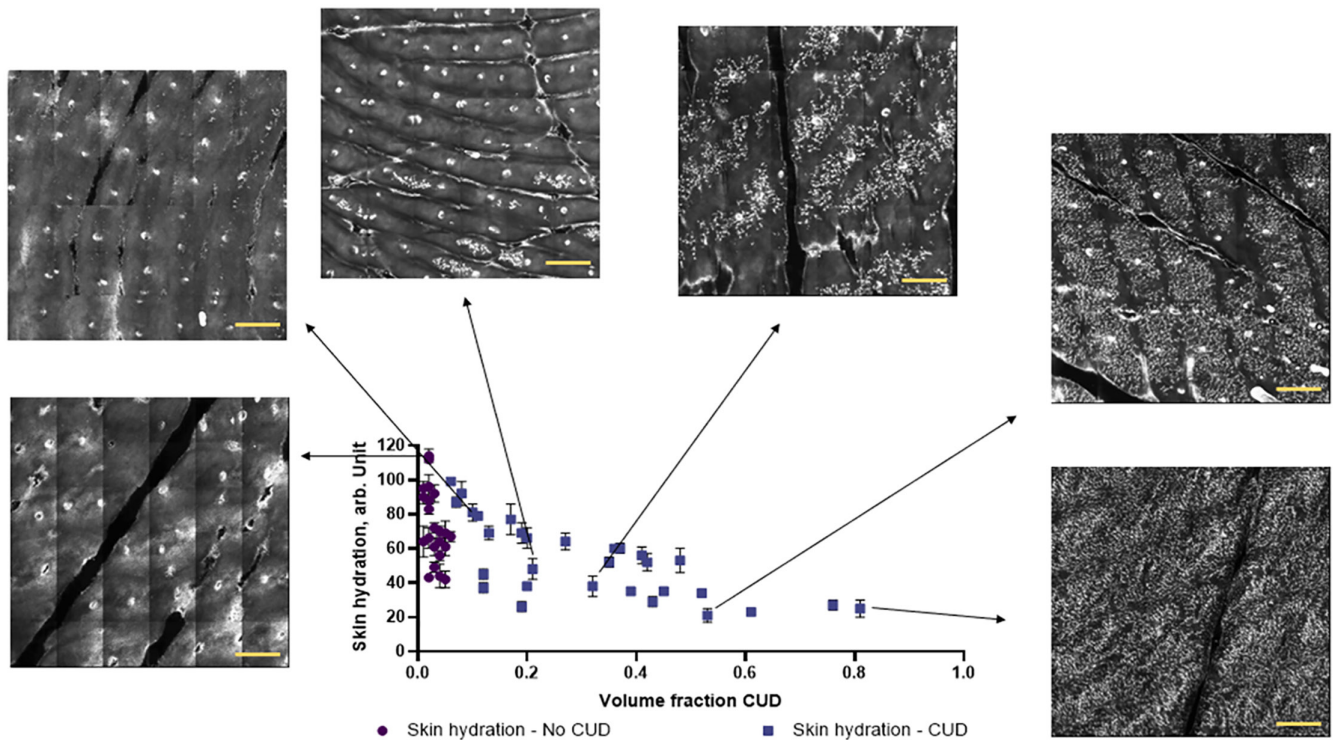


FIGURE 4 SC hydration and the presence of CUD. The maximum volume fraction of CUD structures decreases with increasing skin hydration. Areas of 9 mm² for participants with different volumes of CUD visualize how a higher amount of CUD is related to lower skin hydration values. The yellow bars indicate a scale of 500 μm.

SC depth then determines the possible crystallization depending on the resulting urea saturation. The thick SC seems to be fundamental for the process of crystallization. The urea delivered from the sweat glands may be deposited in the SC and crystallize there. For SC in which the CUD structures were formed, an additional reduction in water concentration can be conceived, when the hygroscopic urea molecules are crystallized and thus lose their moisturizing function.

These results show signs of an irregularity in the water concentration gradient of the SC for the participants with higher amount of CUD, making the superficial SC more favourable for saturation of substances. As the amount of water remains at values below those observed for volunteers without the CUD, we can understand the CUD formation process as directly dependent on SC hydration, being enhanced by the presence of the crystals since the water-binding capacity of urea will be affected. We expect a reduction of the CUD structures after enhancement in skin hydration depending on the moisturizer. The only question is whether this reduction will have a short- or long-term effect.

It is important to emphasize that all measurements were performed in an environment with controlled air temperature and relative humidity (20–22°C and 45%–55%).^{43,44} This is a standard in the application of the techniques in dermatological clinical trials. The glabrous skin does not present any hair, which has already been reported as an interference in corneometer measurements.⁴⁵ Regarding the role of sebum in the present findings, it is important to highlight that we do not have sebaceous glands in the glabrous skin and low amount of sebum is available.⁴⁶ However, we cannot totally

exclude the role of sebum since we are constantly touching our face and other body parts or even from lipid-rich cosmetics.

Since the maintenance of skin hydration levels is fundamental to avoid occupational challenges such as eczema, atopic dermatitis and since the causes of drier hands are not well described, the identification of CUDs offers a novel important approach in dermatology. These results open a new direction to contribute to different perspectives such as the development of better moisturizers or the diagnostic of dry and xerotic skin conditions. Future research involving the presence of CUD in glabrous skin should be directed to the mechanisms exploited by moisturizers that present urea in their composition. Crystallization indicates a saturation in the urea levels, and the utilization of moisturizer creams containing this humectant may not deliver more functional urea to the skin if crystallization occurs after application to the skin, rather being counterproductive. For individuals showing CUD structures, the moisturization by urea could be compromised. Further studies should aim to better understand the presence and distribution of CUDs in the population and to confirm whether CUD structures are signature or cause of dry skin.

AUTHOR CONTRIBUTIONS

V.H.P.I. conducted the study, recruited participants, obtained the images from LSM, made the analysis for all methods, statistics, participated in the discussions and wrote the paper. R.B. was responsible for providing the financial support, formal analyses, supervision, discussions and revised the paper, M.K. has acquired

the 2PM images, performed the analysis, discussed and reviewed the paper, M.C.M. has performed the formal analyses, supervision, discussions, revised the paper and provided the laboratory where the study was performed. M.E.D. performed the Raman and corneometry measures, formal analyses, supervision, discussions and revised the paper.

ACKNOWLEDGEMENTS

We want to thank the financial support provided by the Volkswagen Foundation. Open Access funding enabled and organized by Projekt DEAL.

CONFLICT OF INTEREST STATEMENT

The authors have declared no conflicts of interest for the present work.

DATA AVAILABILITY STATEMENT

The data that support the findings of this study are available on request from the corresponding author. The data are not publicly available due to privacy or ethical restrictions.

REFERENCES

- Koenig K, Speicher M, Bückle R, et al. Kaatz M clinical optical coherence tomography combined with multiphoton tomography of patients with skin diseases. *J Biophotonics*. 2009;2(6-7):389-397.
- Park J, Kim M, Lee Y, Lee HS, Ko H. Fingertip skin-inspired microstructured ferroelectric skins discriminate static/dynamic pressure and temperature stimuli. *Sci Adv*. 2015;1(9):e1500661.
- Gould J. Superpowered skin. *Nature*. 2018;563(7732):84-85.
- Holowka NB, Wynands B, Drechsel TJ, et al. Foot callus thickness does not trade off protection for tactile sensitivity during walking. *Nature*. 2019;571(7764):261-264.
- Yum SM, Baek IK, Hong D, et al. Fingerprint ridges allow primates to regulate grip. *PNAS*. 2020;117(50):31665-31673.
- Shahriari N, Grant-Kels JM, Rabinovitz H, Oliviero M, Scope A. Reflectance confocal microscopy features of melanomas on the body and non-glabrous chronically sun-damaged skin. *J Cutan Pathol*. 2018;45(10):754-759.
- Walcher J, Ojeda-Alonso J, Haseleu J, et al. Specialized mechanoreceptor systems in rodent glabrous skin. *Physiol J*. 2018;596(20):4995-5016.
- Yamazaki Y, Imura M, Nagata N. Tactile presentation scheme based on physiological characteristics of the fingertip. *International Conference on Human-Computer Interaction*. Springer, Cham; 2019:172-179.
- Herrmann DN, Boger JN, Jansen C, Alessi-Fox C. In vivo confocal microscopy of Meissner corpuscles as a measure of sensory neuropathy. *Neurology*. 2007;69(23):2121-2127.
- Elsner P, Agner T. Hand eczema: treatment. *J Eur Acad Dermatol Venereol*. 2020;34:13-21.
- Nam GW, Baek JH, Koh JS, Hwang JK. The seasonal variation in skin hydration, sebum, scaliness, brightness and elasticity in Korean females. *S Res Technol*. 2015;21(1):1-8.
- Baumeister T, Uter W, Weistenhöfer W, Drexler H, Kütting B. On the lookout for precursor lesions: where does dry skin end and slight hand eczema begin? *Contact Derm*. 2012;66(2):63-71.
- Celleno L. Topical urea in skincare: a review. *Dermatol Ther*. 2018;31(6):e12690.
- Piquero-Casals J, Morgado-Carrasco D, Granger C, Trullàs C, Jesús-Silva A, Krutmann J. Urea in dermatology: a review of its emollient, moisturizing, keratolytic, skin barrier enhancing and antimicrobial properties. *Dermatol Ther*. 2021;11(6):1905-1915.
- Starace M, Alessandrini A, Piraccini BM. Clinical evidences of urea at high concentration on skin and annexes. *Int J Clin Pract*. 2020;74:e13740.
- Hadorn B, Hanimann F, Anders P, Curtius HC, Halverson R. Free amino acids in human sweat from different parts of the body. *Nature*. 1967;215(5099):416-417.
- Björklund S, Engblom J, Thuresson K, Sparr E. Glycerol and urea can be used to increase skin permeability in reduced hydration conditions. *Eur J Pharma Sci*. 2013;50(5):638-645.
- Komives GK, Robinson S, Roberts JT. Urea transfer across the sweat glands. *J Appl Physiol*. 1966;21(6):1681-1684.
- André T, Lévesque V, Hayward V, Lefèvre P, Thonnard JL. Effect of skin hydration on the dynamics of fingertip gripping contact. *J R Soc Interface*. 2011;8(64):1574-1583.
- Darvin ME, Richter H, Zhu YJ, et al. Comparison of in vivo and ex vivo laser scanning microscopy and multiphoton tomography application for human and porcine skin imaging. *Quantum Elec*. 2014;44(7):646-651.
- Calzavara-Pinton P, Longo C, Venturini M, Sala R, Pellacani G. Reflectance confocal microscopy for in vivo skin imaging. *Photochem Photobiol*. 2008;84(6):1421-1430.
- Mercurio DG, Jdid R, Morizot F, Masson P, Maia Campos PMBG. Morphological, structural and biophysical properties of French and Brazilian photoaged skin. *Br J Dermatol*. 2016;174(3):553-561.
- Choe C, Schleusener J, Lademann J, Darvin ME. Keratin-water-NMF interaction as a three-layer model in the human stratum corneum using in vivo confocal Raman microscopy. *Sci Rep*. 2017;7(1):1-13.
- Egawa M, Tagami H. Comparison of the depth profiles of water and water-binding substances in the stratum corneum determined in vivo by Raman spectroscopy between the cheek and volar forearm skin: effects of age, seasonal changes and artificial forced hydration. *Br J Dermatol*. 2008;158(2):251-260.
- Caspers PJ, Bruining HA, Puppels GJ, Lucassen GW, Carter EA. In vivo confocal Raman microspectroscopy of the skin: noninvasive determination of molecular concentration profiles. *J Invest Dermatol*. 2001;116(3):434-442.
- Kröger M, Scheffel J, Nikolaev VV, et al. In vivo non-invasive staining-free visualization of dermal mast cells in healthy, allergy and mastocytosis humans using two-photon fluorescence lifetime imaging. *Sci Rep*. 2020;10(1):1-16.
- Kröger M, Schleusener J, Jung S, Darvin ME. Characterization of collagen I fiber thickness, density, and orientation in the human skin In vivo using second-harmonic generation imaging. *Photonics*. 2021;8(9):404.
- Breunig HG, Weinigel M, Bückle R, et al. Clinical coherent anti-stokes Raman scattering and multiphoton tomography of human skin with a femtosecond laser and photonic crystal fiber. *Laser Phys Lett*. 2013;10(2):025604.
- Weinigel M, Breunig HG, Kellner-Höfer M, et al. In vivo histology: optical biopsies with chemical contrast using clinical multiphoton/coherent anti-stokes Raman scattering tomography. *Laser Phys Lett*. 2014;11(5):055601.
- Roth S, Freund I. Second harmonic generation in collagen. *Chem Phys*. 1979;70(4):1637-1643.
- Ledoux I, Zyss J. Influence of the molecular environment in solution measurements of the second-order optical susceptibility for urea and derivatives. *Chem Phys*. 1982;73(1-2):203-213.
- Crosignani V, Jahid S, Dvornikov AS, Gratton E. A deep tissue fluorescence imaging system with enhanced SHG detection capabilities. *Microsc Res Tech*. 2014;77(5):368-373.
- Halbott JM, Blit S, Donaldson W, Tang C. Efficient phase-matched second-harmonic generation and sum-frequency mixing in urea. *IEEE J Quantum Elect*. 1979;15(10):1176-1180.

34. Manju T, Selvarajan P. Investigations on growth and characterization of mono-urea oxalic acid crystals. *IAJER*. 2018;13:11054-11061.
35. Wu JQ, Kilpatrick-Liverman L. Characterizing the composition of underarm and forearm skin using confocal raman pectroscopy. *Int J Cosm Sci*. 2011;33(3):257-262.
36. Egawa M, Sato Y. *In vivo* evaluation of two forms of urea in the skin by Raman spectroscopy after application of urea-containing cream. *S Res Technol*. 2015;21(3):259-264.
37. Albèr C, Brandner BD, Björklund S, Billsten P, Corkery RW, Engblom J effects of water gradients and use of urea on skin ultrastructure evaluated by confocal Raman microspectroscopy. *Biochim Biophys Acta-Biomembr*. 2013;1828(11):2470-2478.
38. Keuleers R, Desseyen HO, Rousseau B, Van Alsenoy C. Vibrational analysis of urea. *J Phys Chem*. 1999;103(24):4621-4630.
39. Goto N, Morita Y, Terada K. Deposits from creams containing 20%(w/w) urea and suppression of crystallization (part 3): novel analytical methods based on Raman spectroscopy for the characterization of deposits and deposition phenomena of creams containing 20%(w/w) urea. *Chem Pharm Bull*. 2016;64(8):1099-1107.
40. Brusilow SW. Evidence for a non-plasma source of urea in sweat. *Nature*. 1967;214(5087):506.
41. Czarnowski D, Górski J, Jóźwiuk J, Boroń-Kaczmarska A. Plasma ammonia is the principal source of ammonia in sweat. *Eur J Appl Physiol*. 1992;65(2):135-137.
42. Allen AE, Dupont CL, Oborník M, et al. Evolution and metabolic significance of the urea cycle in photosynthetic diatoms. *Nature*. 2011;473(7346):203-207.
43. Heinrich U, Koop U, Leneveu-Duchemin MC, et al. Multicentre comparison of skin hydration in terms of physical-, physiological- and product-dependent parameters by the capacitive method (Corneometer CM 825). *Int J Cosm Science*. 2003;25(1-2):45-53.
44. O'goshi KI, Serup J. Inter-instrumental variation of skin capacitance measured with the Corneometer®. *S Res Technol*. 2005;11(2):107-109.
45. Loden M, Hagforsen E, Lindberg M. The presence of body hair influences the measurement of skin hydration with the Corneometer. *Acta Dermato-Venereol*. 1995;75(6):449-450.
46. Firooz A, Sadr B, Babakoochi S, et al. Variation of biophysical parameters of the skin with age, gender, and body region. *Sci World J*. 2012;2012:1-5.

SUPPORTING INFORMATION

Additional supporting information can be found online in the Supporting Information section at the end of this article.

Fig. S1

Fig. S2

Fig. S3

Fig. S4

How to cite this article: Infante VHP, Bennewitz R, Kröger M, Meinke MC, Darvin ME. Human glabrous skin contains crystallized urea dendriform structures in the *stratum corneum* which affect the hydration levels. *Exp Dermatol*. 2023;32:986-995. doi:[10.1111/exd.14802](https://doi.org/10.1111/exd.14802)